ELSEVIER

The Verisimilitude of the Independent Pixel Approximation Used in Cloud Remote Sensing

Alexander Marshak,[*,‡] *Anthony Davis,*[*,§] *Warren Wiscombe,*[*] *and Georgii Titov*[†]

We assess the validity of the "independent pixel approximation" (IPA) using Monte Carlo simulations of realistic scale-invariant clouds modeled with 2-D horizontal variations in optical depth. The IPA uses a plane-parallel approximation for each pixel, and is used in virtually all cloud remote sensing algorithms. We confirm the validity of the IPA at the largest scales and demonstrate its shortcomings on the smallest scales: a) It overestimates the variability of the radiation field when the optical depth field is known, and b) it underestimates the variability of the optical depth field when the radiation field is known. Both effects are due to smoothing by horizontal fluxes.

INTRODUCTION

Not only mean optical depth but also its spatial distribution affects cloud radiative properties (Stephens, 1985; 1986). Lovejoy (1982) showed that cloud shapes are fractal. There is little doubt that this is due to atmospheric turbulence as it is well established that turbulence produces fractal structures (e.g., Mandelbrot, 1982). Together these facts suggest that cloud internal structure can be simulated with fractal models adapted from turbulence theory. Cahalan et al. (1994a) introduced such a fractal cascade model, which simulates the horizontal variability of liquid water observed in marine stratocumulus clouds. The scaling properties of this model were studied in detail by Marshak et al. (1994). For scaling processes, one consequence is power-law behavior of the energy spectrum

$$E(k) \propto k^{-\beta} \tag{1}$$

over a large range of scales $r \approx 1/k$. Cahalan and Snider (1989), and Davis et al. (1994) find power-law spectra of liquid water in marine stratocumulus, with β in the range 1.5–5/3.

Monte Carlo (MC) methods are the simplest numerical tools for studying the radiative properties of inhomogeneous clouds. A rigorous treatment of the MC technique in atmospheric optics can be found in Marchuk et al. (1980). Early 3-D Monte Carlo cloud radiation calculations (McKee and Cox, 1974) focused exclusively on internally homogeneous cubic clouds. Such unrealistic models gave way to applying MC to fractal and multifractal cloud models [Cahalan, 1989; Davis et al., 1990; 1991; Barker and Davies, 1992; Evans, 1993, implementing O'Brien's (1992) backward Monte Carlo; Cahalan et al., 1994b].

For inhomogeneous clouds, Cahalan (1989) proposed the independent pixel approximation (IPA), which approximates the radiation properties of each pixel using plane-parallel radiative transfer theory. When the IPA is valid, the only information needed is the probability of occurrence of a given optical depth, independently of neighboring values. This reduces considerably the computer time needed to calculate accurate cloud albedoes. In essence, a full 3-D radiation calculation is replaced by an ensemble of plane-parallel calculations. Cahalan et al. (1994a,b) apply both MC and IPA to a simple 1-D horizontal fractal model of internal variability for marine stratocumulus clouds, ignoring the effect of cloud shape. Cahalan et al. (1994a) find significant "plane-parallel biases"—differences in domain-averaged albedo using the IPA and plane-parallel theory using

[*]NASA Goddard Space Flight Center, Climate and Radiation Branch, Greenbelt.

[†]Institute of Atmospheric Optics Russian Academy of Sciences, Tomsk, Russia.

[‡]Also Science Systems and Applications, Inc. (SSAI), Lanham, Maryland.

[§]Also Universities Space Research (USRA), NASA-GSFC, Greenbelt.

Address correspondence to Alexander Marshak, Climate & Radiation Br., NASA-GSFC, Code 913, Greenbelt, MD 20771.

Received 5 July 1994; revised 24 December 1994.

REMOTE SENS. ENVIRON. 52:71–78 (1995)

655 Avenue of the Americas, New York, NY 10010

0034-4257/95/$9.50
SSDI 0034-4257(95)00016-T

the domain-averaged optical thickness. Then Cahalan et al. (1994b) assessed MC-to-IPA biases and found them to be relatively small for the domain-averaged radiation properties but large for individual pixels.

In this article we address a question that complements Cahalan et al.'s results for domain-averaged albedo: Does the IPA accurately predict the observed *variability* of the albedo field? Equivalently, we can ask in Preisendorfer's (1978) terms: Does the *apparent* optical depth field (retrieved from the observed albedoes using the IPA) bear any resemblance to the *inherent* optical depth field? We first (in the next section) describe a 2-D scale-invariant bounded cascade model which is a straightforward generalization of the 1-D model of Cahalan et al. (1994a). This model determines the inherent structure of the cloud. In the third section we discuss briefly a 3-D MC method that exploits a variance reduction technique called the Maximal Cross-Section Method and define a simple IPA-based procedure to retrieve the optical depth field from the MC albedoes. This procedure determines the apparent structure of the cloud. Finally, in the fourth section we estimate the accuracy of the IPA and its range of applicability by comparing the smoothness properties of the MC and IPA albedo and optical depth fields.

We adopt here the simplest possible measure of "smoothness": the spectral exponent β in Eq. (1), as determined by linear regression of log $E(k)$ versus log k, all scales (k's) combined. In a more detailed study (Davis et al., 1995), we shall show that, rather than changing this "effective" β, the horizontal fluxes that are responsible for MC-to-IPA differences reduce the range of scales where Eq. (1) applies.

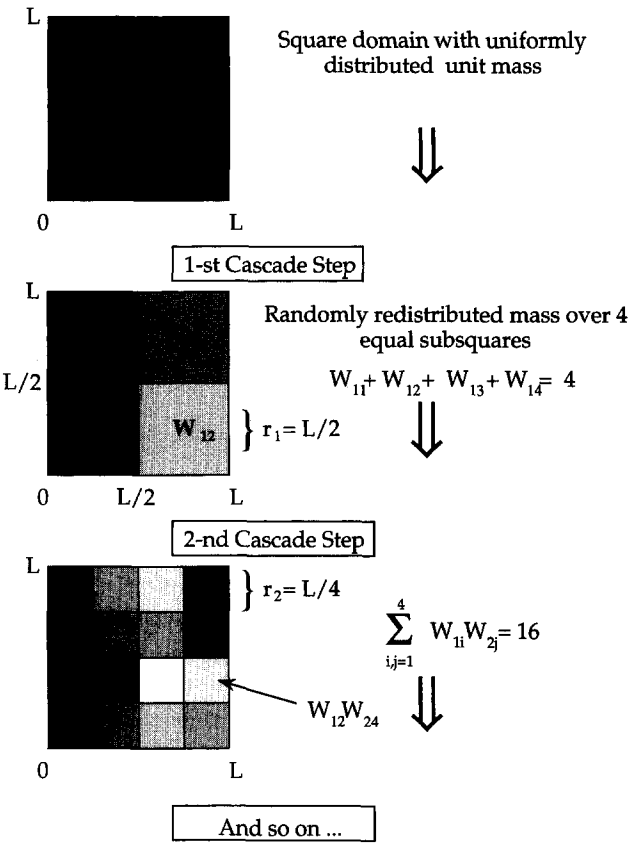

Figure 1. Construction of a mass-conserving 2-D multiplicative cascade model. Starting with a homogeneous square of size $[0,L]\times[0,L]$, one first redistributes the unit mass over four subsquares of equal size. This is equivalent to multiplying the previously uniform density field on each subsquare of side length $r_1 = L/2$ by W_{1j} ($j = 1, \ldots, 4$), where $\sum_{j=1}^{4} W_{1j} = 4$. The same procedure is repeated at smaller scales $r_n = L/2^n$ using weights W_{nj} ($j = 1, \ldots, 4$) for each of 4^n subsquares with $\sum_{j_1,j_2,\ldots,j_n=1}^{4} W_{1j_1}W_{2j_2}\cdots W_{nj_n} = 4^n$, $n > 1$. The case of $n = 2$ is shown on a bottom panel.

INHERENT CLOUD STRUCTURE

Clouds are turbulent environments; we therefore follow accepted phenomenology and simulate clouds with multiplicative cascade models. We will first describe the construction of a 2-D cascade model with random but identically distributed weights and then illustrate the choice of weights for a simple 1-D case. A rigorous formalism for random cascades can be found in Holley and Waymire (1992).

Consider a homogeneously distributed quantity (say optical depth, τ_0) in a square $X = [0,L]\times[0,L]$ (see Fig. 1 with τ_0 equal to 1 for simplicity). First we subdivide X into four subsquares of side length $r_1 = L/2$ and redistribute τ_0 over each of these subsquares as $\tau_0 W_{11}$, $\tau_0 W_{12}$, $\tau_0 W_{13}$, and $\tau_0 W_{14}$, where W_{1j}, ($j = 1, \ldots, 4$) are nonnegative identically distributed random numbers (weights). The distribution must have unit mean so that, averaged over a large number of steps and realizations, the mean of the W's is unity. [For a strictly mass-conserving cascade, the mean of the four W's is forced to unity for every cascade step (as in Fig. 1).] At the next cascade step, each of subsquares is further subdivided into four subsquares of side length $r_2 = L/4$, and the optical depth is again redistributed as $\tau_0 W_{1i} W_{2j}$ ($i,j = 1, \ldots, 4$) over all 16 subsquares. Proceeding iteratively, at the nth step the original square X is divided into 4^n subsquares of side length $r_n = L/2^n$ and the optical depth of each subsquare τ_n is given by the product of τ_0 and n weights W_{ij} ($i = 1, \ldots, n$), where index j randomly takes one of its four values. After n iterations, the 4^n subsquares of area $r_n \times r_n$ are assumed homogeneous (small scale homogeneity assumption), and the overall average $\langle \tau_n \rangle = \tau_0$.

If $n \to \infty$, the optical depth of an individual subsquare τ_n may or may not be bounded depending on the distribution from which the W's are selected. Unbounded or "singular" cascade models will have $\tau_n \to 0$ for almost all cells as $n \to \infty$, since $\langle \tau_n \rangle = \tau_0$ for any n. Bounded cascade models have upper and lower bounds: $0 < \tau_{\min} \leqslant \lim_{n\to\infty} \tau_n \leqslant$

$\tau_{max} < \infty$. To make a cascade model bounded, it is necessary (but not sufficient) that the W's $\to 1$ as $n \to \infty$ (Marshak et al., 1994), that is, the distribution from which the W's are drawn must become more and more centered around unity as $n \to \infty$.

For vertically integrated liquid water in stratocumulus, Cahalan et al. (1994a) use a 1-D two-parameter bounded cascade model with weights $W_n = 1 \pm (1-2p)/2^{(n-1)H}$, at scale $r_n = L/2^n$, where "$\pm$" means that the weights $1+(1-2p)/2^{(n-1)H}$ and $1-(1-2p)/2^{(n-1)H}$ are taken with equal probability. The parameter p $(0<p<1/2)$ controls the variance-to-mean ratio of the cloud liquid water distribution and the parameter $H \geq 0$ defines its scaling behavior. If $H=0$, we retrieve Meneveau and Sreenivasan's (1987) "p-model," a singular cascade model originally designed to simulate the dissipation field in turbulence. As soon as $H>0$, the distributions of W's contracts around unity as $n \to \infty$, as required for a bounded model, and (Cahalan et al., 1994a),

$$\frac{\tau_{max}}{\tau_0} < \exp\left[\frac{2^H(1-2p)}{2^H-1}\right] < \infty. \tag{2}$$

The spectral exponent β in the limit of $n \to \infty$ shows different behavior for singular $(H=0)$ models

$$0 < \beta = -\log_2[1-2p(1-p)] < 1, \tag{3a}$$

and bounded $(H>0)$ models,

$$1 < \beta = \min\{2H,1\} + 1 \leq 2, \tag{3b}$$

the last result being independent of p (Marshak et al., 1994). Setting $H=1/3$ yields $\beta = 5/3$, as observed for stratocumulus liquid water path from a microwave radiometer (Cahalan and Snider, 1989).

A simple 2-D generalization of the above 1-D mass-conserving bounded model gives us a three-parameter model with weights

$$\begin{cases} W_{n1} = 1+(1-2p_1)/2^{(n-1)H}, & W_{n2} = 2-W_{n1}, \\ W_{n3} = 1+(1-2p_2)/2^{(n-1)H}, & W_{n4} = 2-W_{n3}, \end{cases}$$

which are taken randomly with equal probability, that is, the probability distribution is just a sum of four δ-functions, at these four values. Figure 2a illustrates a realization of this model with $H=1/3$ and $n=7$ (128×128 pixels), where $p_1 = 0.26$ and $p_2 = 0.34$. (To estimate the upper bound τ_{max} in 2-D case, one can use Eq. (2) with $p = \min\{p_1,p_2\}$.) Setting the mean vertical optical depth $\tau_0 = 12$ gives a range of optical depth from 1.4 to 65.1. The parameters remaining to be defined are the geometrical vertical (h) and horizontal (L) sizes. Since marine stratocumulus are typically 200–400 m thick, we take $h = 300$ m in the vertical and, to get a pixel size near the size of a Landsat pixel (30 m), we take $r_n = 50$ m (hence overall horizontal size $L = 128 \times 50$ $m = 6.4$ km). We apply cyclical boundary conditions to emulate a large horizontal extention. Thus our cloud can be viewed as a stratocumulus deck, 300 m thick and 6.4 km on a side for the basic element; the mean extinction coefficient $\sigma_{mean} = 13/0.3 = 43\ km^{-1}$; the mean single-pixel horizontal optical thickness $\tau_{pix} = \sigma_{mean} r_n = 2.2$; and the total horizontal optical thickness per basic element $\tau_h = 128\tau_{pix} = 277$.

CALCULATION OF APPARENT CLOUD PROPERTIES

Monte Carlo

The MC method applied to the above optical depth model is a forward one which tracks photons from their source to their eventual exit. However, in order to reduce MC noise, we do not use a direct method but rather simulate photon histories that differ from the physical ones. Among the large number of variance reduction techniques developed mostly for neutron transport, we use a lesser known one called maximal cross-section method (Marchuk et al., 1980). It involves transforming the radiative transfer equation for multiple scattering from

$$\boldsymbol{\Omega}\cdot\nabla I(r,\boldsymbol{\Omega}) + \sigma(r) I(r,\boldsymbol{\Omega}) = \varpi_0(r)\sigma(r)\int_{4\pi} P(\boldsymbol{\Omega}\cdot\boldsymbol{\Omega}') I(r,\boldsymbol{\Omega}')\, d\boldsymbol{\Omega}' \tag{4a}$$

to

$$\boldsymbol{\Omega}\cdot\nabla I(r,\boldsymbol{\Omega}) + \sigma_{max} I(r,\boldsymbol{\Omega}) = \sigma_{max}\int_{4\pi}\left\{\frac{\sigma(r)}{\sigma_{max}}\varpi_0(r)P(\boldsymbol{\Omega}\cdot\boldsymbol{\Omega}') + \left[1-\frac{\sigma(r)}{\sigma_{max}}\right]\delta(\boldsymbol{\Omega}-\boldsymbol{\Omega}')\right\} I(r,\boldsymbol{\Omega}')\, d\boldsymbol{\Omega}' \tag{4b}$$

where $\sigma_{max} = \max_{\text{all } r} \sigma(r)$ is the maximal extinction, ϖ_0 is the single scattering albedo, and P is the angular scattering probability distribution or phase function. Equation (4b) can be interpreted as the transport equation with constant extinction and a modified phase function equal to $\varpi_0(r)P(\boldsymbol{\Omega},\boldsymbol{\Omega}')$ with probability $\sigma(r)/\sigma_{max}$ and $\delta(\boldsymbol{\Omega}-\boldsymbol{\Omega}')$ otherwise (like the δ-Eddington method but position-dependent). This method allows each photon to jump immediately to its next scatter point rather than accumulating optical depth cell-by-cell. This makes MC code computer time almost insensitive to 1) whether we use 1-D, 2-D, or 3-D geometry, 2) the variability of $\sigma(r)$ except for very large σ_{max}, and 3) the number of cells. All three of these substantially slow down straightforward MC in inhomogeneous media. The above technique is very economical: For fractal clouds simulated on a 128×128 grid, we were able to run 100 million photons in 20 h on an HP/9000 workstation; this is sufficient to give better than 1% accuracy in every pixel for cloud fluxes in albedo and in transmittance.

Figure 3a shows cloud albedo R_{MC} for a 128×128 grid calculated by our Monte Carlo code with 10^8 photons and no absorption $[\varpi_0(r) \equiv \varpi_0 = 1]$. Solar zenith angle

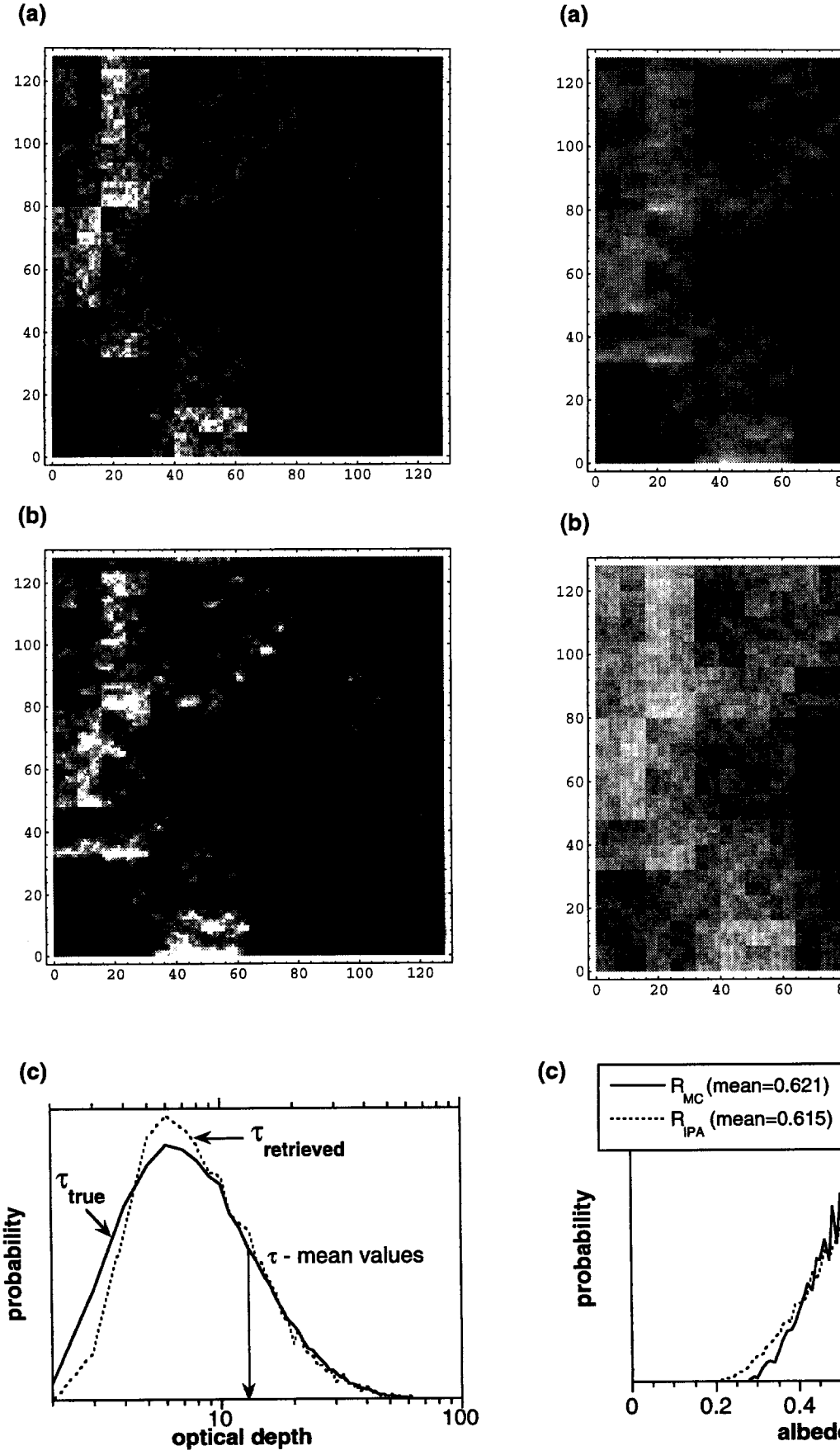

Figure 2

Figure 3

is 60°, and the cloud is illuminated from the top of the image; the phase function is Henyey and Greenstein's (1941) with asymmetry factor $g = 0.843$ (typical for scattering by cloud droplets at wavelengths 0.3–1 μm).

Although remote sensing is based on radiances rather than fluxes, we will continue to use albedo as a surrogate for radiance measured by a nadir-looking instrument. In an upcoming study (Davis et al., 1995), we shall show that the two fields are closely related, at least in the class of clouds models under consideration here.

Optical Depth Retrievals in the Independent Pixel Approximation

The independent pixel approximation (IPA) assumes that the reflectivity of each cloud pixel depends only on its own optical depth and not on the optical depth of neighboring pixels (Cahalan, 1989; Cahalan et al., 1994a; Cahalan, 1994). In other words, the IPA uses a 1-D plane-parallel approach for each pixel and neglects any *net* horizontal photon transport.

To simulate an IPA, we used a 1-D albedo approximation, R_{IP} derived by Cahalan et al. (1994a) for conservative scattering:

$$R_{IP}(\tau;\theta,g) = 1 - T_{IP}(\tau;\theta,g),$$

$$T_{IP}(\tau;\theta,g) = \frac{\delta(\theta) + [1 - \delta(\theta)]\exp[-\tau/|a(\theta)|]}{1 + \gamma(g)\tau}, \quad (5)$$

where T_{IP} is transmittance, τ is the cloud optical depth, θ is the solar zenith angle, and g is the asymmetry factor. We use the following values of the functions $\delta(\theta)$, $a(\theta)$, and $\gamma(g)$: $\delta(60°) \approx 0.8$, $a(60°) \approx 2.6$, $\gamma(0.843) \approx 0.11$. Applying Eq. (5) to the vertical depth field in Figures 2a yields the R_{IP} field in Figure 3b.

To retrieve the vertical optical depth field from MC cloud albedo R_{MC}, we replace R_{IP} by R_{MC} in Eq. (5) and solve it for τ using Newton's method. Since R_{MC} unlike R_{IP}, is not necessarily smaller than unity (it is possible for more energy to leave a pixel than enters it), we have to assume a cutoff for the retrieved τ: Individual pixel values cannot exceed some large number, for example, the one defined in Eq. (2), approximately 100. (There are 60 pixels out of $128^2 = 16{,}384$ that have albedo larger than $R_{IP}(100; 60°, 0.843) = 0.933$.) Figure 2b illustrates the resulting retrieved optical depth field.

COMPARATIVE SPECTRAL ANALYSIS OF INHERENT AND APPARENT FIELDS

MC versus IPA, Original (Inherent) versus Retrieved (Apparent) Optical Depth Fields

Figures 3a and 3b show two albedo fields calculated by MC and IPA, respectively, for the modeled optical depth field in Figure 2a. Since IPA computations depend only on the local pixel properties, they are accurate when all pixels have large horizontal optical depth, and therefore few photons are exchanged between pixels, relative to the number which exit the top and bottom of each pixel. But, in our example, a mean single-pixel horizontal optical depth, τ_{pix}, is only about 2 photon mean free paths and there is a dramatic difference between R_{MC} and R_{IP} for individual pixels. However, the domain-averaged albedoes are very close (within 1%) which is typical for stratocumulus clouds (Cahalan et al., 1994b). The histograms for R_{MC} and R_{IP} are also plotted in Figure 3c; apart from the nonvanishing probability of having $R_{MC} \geq 1$, they look very similar.

MC albedo (Fig. 3a) is much smoother, visually, than its IPA counterpart (Fig. 3b). Similarly, our simple IPA retrieval procedure from MC albedo yields a much smoother optical depth field (Fig. 2b) than the original (Fig. 2a). The energy spectra in Figure 4 confirm our

Figure 4. Energy spectra. For the optical depth in Figure 2a and the IPA-retrieved optical depth field in Figure 2b (top); for the MC and IPA albedo fields in Figures 3a and 3b, respectively (bottom).

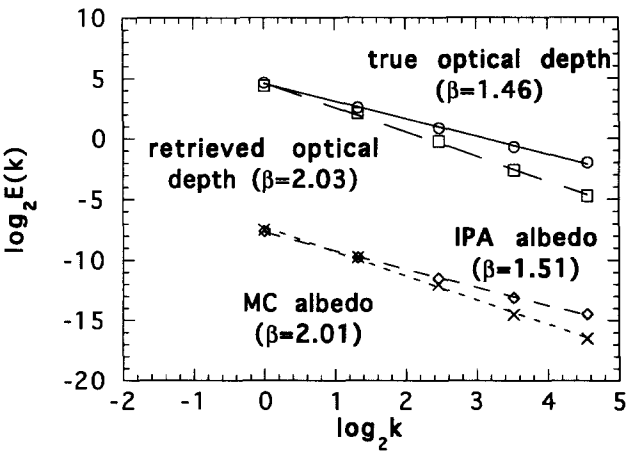

Figure 2. 2-D Optical depth fields. a) 2-D bounded cascade model with $n = 7$ cascade steps, $\tau_0 = 13$ (see Cahalan et al., 1994a), $H = 1/3$ ($\beta = 5/3$ for $n = \infty$), $p_1 = 0.26$, and $p_2 = 0.34$ [see Cahalan (1994c) with different notations]; the range of vertical optical depth is from 1.4 to 65.1. The dense regions are white, the least dense regions black. The shade of gray is linear in the pixel value. b) Optical depth retrieved from MC albedo in Figure 3a using Eq. (5) as an IPA; its mean value is 13.56, close to τ_0; the range of retrieved τ is from 2.0 to 100. c) Histograms for the two optical depth fields in a) and b).

Figure 3. 2-D Albedo fields. a) MC albedo R_{MC} for Figure 2a, sun at $\theta = 60°$, $\varphi = 0°$; no absorption, Henyey–Greenstein phase function with $g = 0.843$, 10^8 photons, $\langle R_{MC} \rangle = 0.621$. The shade of gray is linear in the pixel value. b) Albedo field R_{IP} using the IPA formula $R(60°,\tau) = 1 - [0.8 + 0.2\exp(-\tau/2.6)]/(1 + 0.11\tau)$ with τ from Figure 2a; $\langle R_{IP} \rangle = 0.615$. c) Histograms for the two albedo fields in a) and b). Notice the small but finite probability of $R_{MC} \geq 1$.

visual impressions. We know that, in the limit of an infinite number of cascade steps, the bounded model with $H = 1/3$ gives $\beta = 5/3$ [Eq. (3b)]; in the present case of seven cascades we find $\beta = 1.46$ while the retrieved optical depth gives $\beta \approx 2$. IPA albedo has $\beta = 1.51$, while MC albedo shows a much smoother behavior with β slightly larger than 2.

2-D MC Calculations, Three Case Studies in Scaling

To study the smoothing effect of radiation on the horizontal distribution of the optical depth in cloud fields, it is not absolutely necessary to use a 2-D model of optical depth; a 1-D model will provide us with similar information. Having scale-invariant models in mind, the advantage of a 1-D model is evident: For the same computer time, we can access a larger range of scales than in the 2-D case. For example, instead of a 128×128 grid with only a two-decade range of scales, we can use a $16{,}384 \times 1$ grid with a 4-decade range of scales. So, let us assume that clouds are now fractal in one horizontal direction and uniform in the other horizontal direction as well as in the vertical, as in Cahalan et al. (1994a).

Another simplification is to use 2-D MC radiation calculations instead of 3-D ones. In this case the photons are confined to the x–z plane where the horizontal direction x is a fractal (1-D bounded model) and the vertical direction z is uniform. The 2-D analogue of the Henyey–Greenstein phase function $P(\theta)$ with asymmetry factor g is (Davis et al., 1989)

$$P(\theta) = \frac{1 - g^2}{1 + g^2 - 2g\cos\theta}, \quad -\pi \leqslant \theta \leqslant \pi, \quad \int_{-\pi}^{\pi} P(\theta)\, d\theta = 1. \tag{6}$$

(Notice that there is no exponent 3/2 in the denominator!) Although 2-D and 3-D radiative transfer are mathematically distinct problems, running 2-D and 3-D MC codes on the same 1-D distribution of optical depth yields good agreement in the albedo and transmittance fields (the difference of about 0.5% was even lower than the MC per-pixel noise). We favor the 2-D MC code because: 1) It runs faster (about 10%); 2) a photon trajectory is more easily traceable on a 2-D plane than in 3-D space; 3) as will be shown elsewhere, it allows us to compute the complete distribution of radiance using forward MC. In the three examples below we made 2-D MC calculations with Henyey–Greenstein phase function ($g = 0.843$) defined in Eq. (6), for a single realization of Cahalan's 1-D bounded model with 10 cascade steps, $p = 0.25$ and $H = 1/3$.

We first vary the single scattering albedo ϖ_0. It is well known that albedo is a strong function of ϖ_0 in plane-parallel theory; we show here how the *smoothness* of the albedo field depends also on ϖ_0. Radiation smoothes the albedo field relative to the optical depth field (cf. Figs. 2a and 3a) because of multiple scattering. As ϖ_0 decreases, the contribution of multiple scattering to the albedo field decreases also. Since our optical depth model is scale-invariant, the spectral component β in Eq. (1) is the appropriate quantifier of the albedo field's smoothness. Figure 5 illustrates the dependence of β on $(1 - \varpi_0)^{1/2}$ for ϖ_0 from 0.9 to 1.0, which covers the range of values expected in terrestrial clouds in the visible and near infrared. [The inset in Fig. 5 shows the scaling on a log–log plot of $E(k)$ versus k for four different ϖ_0's.] We see that β decreases from almost 2.2 for $\varpi_0 = 1.0$ to 1.7 for $\varpi_0 = 0.9$ (the optical depth field has $\beta \approx 1.6$). This tells us that the IPA is accurate on a per-pixel basis only at very strongly absorbing wavelengths.

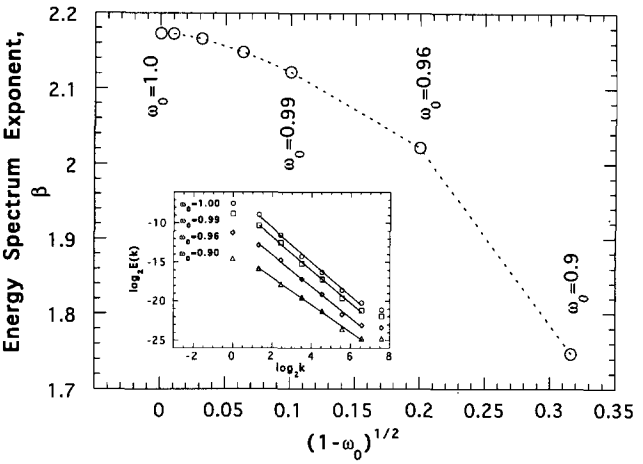

Figure 5. Energy spectra of MC albedo fields for different single scattering albedoes. A 1-D distribution of optical depth was simulated by a bounded model with 10 cascade steps; $\tau_0 = 13$, $p = 0.25$, and $H = 1/3$. The aspect ratio is 30. The results are for 2-D MC: sun in zenith, 2-D Henyey-Greenstein phase function in Eq. (6) with $g = 0.843$, 10^7 photons, ϖ_0 takes the values 1.0, 0.9999, 0.999, 0.996, 0.99, 0.96, and 0.9. The inset shows a double-log plot of $E(k)$ versus k for four different ϖ_0's; slopes yield exponents β. Note that the two points corresponding to the smallest scales (MC noise) and the largest scale (poor statistics with just one realization) were not used in the linear regressions.

We next vary the pixel aspect ratio, defined as the ratio of vertical to horizontal sizes for a single cell. This ratio plays an essential role in comparisons between MC and IPA. Small aspect ratios bring each cell closer to the plane-parallel case, where the IP assumption becomes exact, while large aspect ratios lead to dramatic differences in individual pixel values. In Figure 6, β is plotted against aspect ratio. Keeping the vertical size h of the cloud constant at 300 m, we have changed the horizontal pixel size from 600 m (aspect ratio 0.5, $\tau_{pix} = 26$) to 10 m (aspect ratio 30, $\tau_{pix} = 0.43$). As expected, β sharply increases and levels off at an aspect ratio around 10, which corresponds to a mean single-pixel horizontal optical thickness, τ_{pix}, of about 1 (pixel's size r_n, is about 1 photon mean free path). The two straight lines below

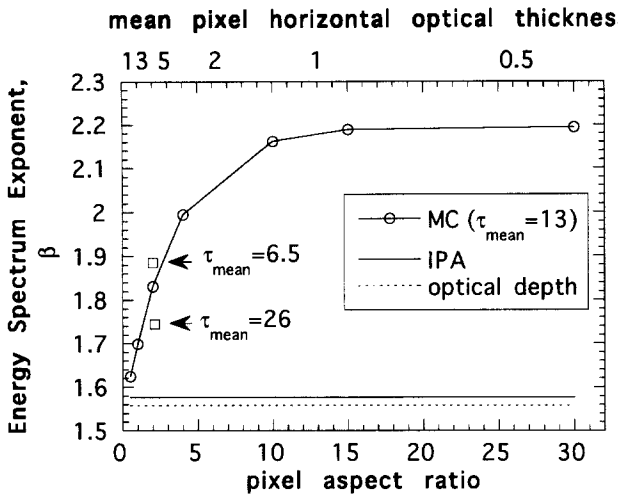

Figure 6. Energy spectra of MC albedo fields or different aspect ratios. MC simulations for a 1-D distribution of optical depth with the same parameters as in Fig. 5 but $\varpi_0 = 1$ and the aspect ratio varies from 0.5 to 30, corresponding to a range of mean single-pixel horizontal optical thickness, τ_{pix}, from 26 to 0.4. The two horizontal lines indicate β values for the R_{IP} field (independent of aspect ratio) and for the optical depth field itself, equal to 1.58 and 1.56, respectively. The two squares at aspect ratio 2 show β values for the two average optical depths: $\tau_0 = 6.5$ and $\tau_0 = 26$. They are equal to 1.89 and 1.75, respectively.

indicate the values of β for both IPA the albedo field ($\beta \approx 1.58$) and the optical depth field ($\beta \approx 1.56$). This tells us that, in absence of absorption, the IPA is accurate on a per-pixel basis only when the cloud pixels are individually opaque in all horizontal directions.

Barker and Davies (1992) argued that multiple scattering has a minor effect on the energy spectrum of the albedo field because it is insensitive to the average vertical optical depth τ_0. They found similar energy spectra for reflected radiation at three different τ_0's (10, 20, and 50). This is consistent with our results since their τ_{pix} varied from 0.08 to 0.4 for a fixed aspect ratio of 128. However, if we consider optically thick pixels (thicker than 1 photon mean free path), the change of τ_0 substantially effects the albedo field. If we fix the aspect ratio at 2 and compare the three τ_0's, 6.5, 13, and 26, we find that the smaller average optical depth yields the smoother albedo field ($\beta \approx 1.9$ for $\tau_0 = 6.5$ versus $\beta \approx 1.75$ for $\tau_0 = 26$). Two square symbols in Figure 6 show these values of β. If, on the contrary, τ_{pix} is held constant, say at 3, we find that the abledo field with $\tau_0 = 13$ ($\beta \approx 2.0$) is smoother than the one with $\tau_0 = 6.5$ ($\beta \approx 1.9$). The explanation is simple: For a given τ_{pix}, increasing τ_0 stretches the length of the vertical interface between columns; this enhances the horizontal photon transport. This tells us that for optically thin pixels, increasing τ_0 has a minor effect on the energy spectrum of the albedo field while, for optically thick pixels with fixed τ_{pix}, increasing τ_0 leads to a smoother albedo field.

SUMMARY AND DISCUSSION

We use a 2-D generalization of Cahalan et al.'s (1994a) 1-D bounded cascade model for the horizontal optical depth distribution in stratocumulus-type clouds. Both 3-D Monte Carlo (MC) and the independent pixel approximation (IPA) were applied to a single realization of this 2-D bounded model (Fig. 2a) to compute the albedo fields (Figs. 3a, b). The maximal cross-section variance reduction technique is used to make the MC code independent of the number of dimensions, the variability of optical depth, and the number of cells. A simple IPA retrieval procedure allows us to estimate the optical depth field from the MC albedo field; the retrieved field (Fig. 2b) is much smoother than the original one (Fig. 2a).

The spectral parameter β, defined operationally in Eq. (1), can be used to compare quantitatively the smoothness of the radiation fields calculated by MC and IPA as well as the original and IPA retrieved optical depth fields. In remote sensing applications, we are interested in the pixel-by-pixel accuracy of the IPA, which is measured to a first approximation by how well the β's agree for albedoes and / or optical depths. In our 2-D simulations of optical depth field, we found a spectral exponent $\beta \approx 1.5$ for both the optical depth field and the IPA albedo field, while the MC albedo field and the optical depth field retrieved from it have $\beta \approx 2$ (Fig. 4).

Three sensitivity studies were also performed: the single scattering albedo ϖ_0, the pixel aspect ratio, and the average optical depth τ_0 were varied. As expected, β is a sensitive function of both the single scattering albedo and the aspect ratio and is determined largely by the horizontal photon transport. As the aspect ratio increases (pixels become horizontally thinner), more and more neighboring pixels become "aware" of each other by exchanging photons in different amounts in the different horizontal directions. This smoothes the radiation fields and β increases, up to an aspect ratio corresponding to a single-pixel horizontal thickness of about one photon mean free path on average (Fig. 6). In addition to being a monotonic function of the aspect ratio, β decreases with the single scattering albedo ϖ_0 (Fig. 5), because absorption also inhibits net horizontal photon transport. Finally, the sensitivity of β to the variation of the average vertical optical depth τ_0 was studied. We found that, when pixels are optically thin on average (smaller than a typical photon free path), β is insensitive to changes in τ_0 while, for optically thick pixels, increasing τ_0 leads to smoother albedo fields (Fig. 6).

In summary, we have used spectral analysis to strongly caveat Cahalan et al. (1994a,b) implication that the

IPA is an accurate way of evaluating cloud radiation properties, even within the framework of unbroken stratus-type cloud fields. We find that the IPA does well at large scales but generally predicts the wrong pixel-to-pixel correlations in the albedo field when the scattering is conservative or almost conservative. Since the IPA is an essential ingredient in cloud optical depth retrievals from satellite and aircraft radiometry (e.g., Nakajima and King, 1990), we recommend using exclusively wavelength channels with strong absorption when pixels sizes are small (less than 100 m).

This work was supported by the Department of Energy's Atmospheric Radiation Measurement (ARM) Project, Grant DE-A105-90ER61069 to NASA's Goddard Space Flight Center. We thank H. Barker, R. Cahalan, P. Gabriel, S. Gollmer, W. Ridgway, and S.-C. Tsay for helpful discussions.

REFERENCES

Barker, H. W., and Davies, J. A. (1992), Cumulus cloud radiative properties and the characteristics of satellite radiance wavenumber spectra, *Remote Sens. Environ.* 42:51–64.

Cahalan, R. F. (1989), Overview of fractal clouds, *Advances in Remote Sensing Retrieval Methods*, Deepak, pp. 371–388.

Cahalan, R. F. (1994), Bounded cascade clouds: albedo and effective thickness, *Nonlin. Process. Geophys.* 1:156–167.

Cahalan, R. F., and Snider, J. B. (1989), Marine stratocumulus structure, *Remote Sens. Environ.* 28:95–107.

Cahalan, R. F., Ridgway, W., Wiscombe, W. J., Bell, T. L., and Snider, J. B. (1994a), The albedo of fractal stratocumulus clouds, *J. Atmos. Sci.* 51:2434–2455.

Cahalan, R. F., Ridgway, W., Wiscombe, W. J., Golmer, S., and Harshvardhan (1994b), Independent pixel and Monte Carlo estimates of stratocumulus albedo, *J. Atmos. Sci.* 51: 3776–3790.

Davis, A., Gabriel, P., Lovejoy, S., and Shertzer, D. (1989), Scaling laws for asymptotically thick clouds dimensional dependence–phase function independence, in *Proceedings of the IRS'88* (J. Lenoble and J. F. Geleyn, Eds.), Deepak, pp. 103–106.

Davis, A., Gabriel, P., Lovejoy, S., Schertzer, D., and Austin, G. (1990), Discrete angle radiative transfer. III. Numerical results and meteorological applications, *J. Geophys. Res.* 95:11,729–11,742.

Davis, A., Lovejoy, S., and Schertzer, D. (1991), Discrete angle radiative transfer in multifractal medium, *SPIE Proc.* 1558:37–59.

Davis, A., Marshak, A., Wiscombe, W., and Cahalan, R. (1994), Multifractal characterizations of non-stationarity and intermittency in geophysical fields, observed, retrieved or simulated, *J. Geophys. Res.* 99:8055–8072.

Davis, A., Marshak, A., and Wiscombe, W. (1995), A mechanism for the scale break observed in Landsat imagery, forthcoming.

Evans, K. F. (1993), Two-dimensional radiative transfer in cloudy atmospheres: the spherical harmonic spatial grid method, *J. Atmos. Sci.* 50:3111–3124.

Henyey, L. C., and Greenstein, J. L. (1941), Diffuse radiation in the galaxy, *Astrophys. J.* 93:70–83.

Holley, R., and Waymire, E. C. (1992), Multifractal dimensions and scaling exponents for strongly bounded random cascade, *Ann. Appl. Probab.* 2:819–845.

Lovejoy, S. (1992), Area–perimeter relation for rain and clouds areas, *Science* 216:185–187.

Mandelbrot, B. B. (1982), *The Fractal Geometry of Nature*, Freeman, New York.

Marchuk, G., Mikhailov, G., Nazaraliev, M., Darbinjan, R., Kargin, B., and Elepov, B. (1980), *The Monte Carlo Methods in Atmospheric Optics*, Springer-Verlag, New York.

Marshak, A., Davis, A., Cahalan, R., and Wiscombe, W. (1994), Bounded cascade models as non-stationary multifractals, *Phys. Rev. E.* 49:55–69.

McKee, T. B., and Cox, S. K. (1974), Scattering of visible radiation by finite clouds, *J. Atmos. Sci.* 31:1885–1892.

Meneveau, C., and Sreenivasan, K. R. (1987), Simple multifractal cascade model for fully developed turbulence, *Phys. Rev. Lett.* 59:1424–1427.

Nakajima, T., and King, M. D. (1990), Determination of the optical thickness and effective particle radius of clouds from reflected solar radiation measurements. I. Theory, *J. Atmos. Sci.* 47:1878–1893.

O'Brien, D. M. (1992), Accelerated quasi-Monte Carlo integration of the radiative transfer equation, *J. Quant. Spectrosc. Radiat. Transfer* 48:41–59.

Preisendorfer, R. W. (1978), *Hydrological Optics*, NOAA, PMEL, Hawaii, Vol. 1.

Stephens, G. L. (1985), Reply (to Harshvardan and Randall), *Mon. Wea. Rev.* 113:1834–1835.

Stephens, G. L. (1986), Radiative transfer in spatially heterogeneous, two-dimensional anisotropically scattering media, *J. Quant. Spectrosc. Radiat. Transfer* 36:51–67.